

Nonlinear hopping transport in ring systems and open channels

Mario Einax,^a Martin Körner,^a Philipp Maass^{*b} and Abraham Nitzan^c

Received 14th August 2009, Accepted 8th October 2009

First published as an Advance Article on the web 18th November 2009

DOI: 10.1039/b916827c

We study the nonlinear hopping transport in one-dimensional rings and open channels. Analytical results are derived for the stationary current response to a constant bias without assuming any specific coupling of the rates to the external fields. It is shown that anomalous large effective jump lengths, as observed in recent experiments by taking the ratio of the third-order nonlinear and the linear conductivity, can occur already in ordered systems. Rectification effects due to site energy disorder in ring systems are expected to become irrelevant for large system sizes. In open channels, in contrast, rectification effects occur already for disorder in the jump barriers and do not vanish in the thermodynamic limit. Numerical solutions for a sinusoidal bias show that the ring system provides a good description for the transport behavior in the open channel for intermediate and high frequencies. For low frequencies temporal variations in the mean particle number have to be taken into account in the open channel, which cannot be captured in the more simple ring model.

1. Introduction

Particle transport in one-dimensional systems is of vital interest for many problems in physics and biology. A prominent example is electron or hole transport in the operation of conducting nanowires, including molecular wires.¹ In such systems transport can be dominated by quantum mechanical tunneling or band motion (the coherent transport limit) but many systems belong to the hopping transport limit, where conduction is a manifestation of a succession of many incoherent hopping steps.^{2,3} For example, both conduction mechanisms were observed in different DNA sequences.⁴ A one-dimensional hopping motion is also the decisive transport mechanism in ion conduction through membrane channels^{5–7} and in unidirectional motion of motor proteins along filaments.^{8,9} Associated with the latter example are recent extensive discussions of boundary driven phase transitions in one-dimensional lattice gases with site exclusion and asymmetric hopping dynamics, commonly referred to as “asymmetric site exclusion processes” (ASEP), or, in case of unidirectional transport, as “totally asymmetric site exclusion processes” (TASEP)—for reviews, see ref. 10–12. Related models were recently applied¹³ to describe the transport of single-stranded DNA segments through nanochannels.¹⁴

The treatment of one-dimensional systems is moreover frequently used as a starting point for describing transport processes in higher dimensions, since it often yields analytical results. In transferring essential results to higher dimensions one has, however, to be careful. An example is the tracer diffusion in one-dimensional hard-core lattice gases, which

exhibits a subdiffusive behavior for long times that originates from the fact that particles cannot pass each other in one dimension.^{15–17}

In this work we study thermally activated hopping conduction in one-dimensional lattices for non-interacting particles in arbitrary energy landscapes. In particular we consider nonlinear transport in strong static and periodic fields. For couplings $\propto \exp(\pm u/2)$ of the external bias u to the bare hopping rate, this problem was first studied for ring systems (periodic boundary conditions) in ref. 18. An exact result for the stationary current was derived, in generalization of an analogous treatment for Brownian dynamics.¹⁹ As a particularly interesting feature, rectification effects were shown to be present for energy landscapes with site energy disorder.

The problem got renewed interest recently for describing measurements on thin glassy electrolytes under high voltages,^{20–23} which allow one to reach the weak nonlinear regime, $u = qEa/k_{\text{B}}T \simeq 1$, where q , a , E , and $k_{\text{B}}T$ are, respectively, the charge of the mobile ions, the typical hopping distance of ($\sim 2\text{--}3$ Å), the applied electric field, and the thermal energy. Molecular dynamics simulations suggest that for these field strengths the influence of the applied field can be applied solely to the mobile ion dynamics, while the effect on the host network structure is negligible.²⁴ In the experiments no rectification was observed so far, implying that the current is an odd function of the applied field. On the other hand, these measurements can be used to determine an effective length scale a_{eff} associated with the ratio σ_3/σ_1 between the third order nonlinear conductivity σ_3 and the linear conductivity σ_1 (cf. eqn (17) below). This length a_{eff} appears to be unphysically large if it is compared to typical jump lengths $a \simeq 2\text{--}3$ Å. Such comparison is motivated by the result²⁵ $j_{\text{dc}} \propto \sinh(qEa/2k_{\text{B}}T)$, derived for the simplest situation of single-particle hopping in an ordered system with the aforementioned coupling, $\propto \exp(\pm u/2)$, of the bias to the bare

^a Institut für Physik, Technische Universität Ilmenau, 98684 Ilmenau, Germany. E-mail: mario.einax@tu-ilmenau.de

^b Fachbereich Physik, Universität Osnabrück, Barbarastraße 7, 49069 Osnabrück, Germany. E-mail: pmaass@uos.de; Fax: +49-541-969-2351; Tel: +49-541-969-2692

^c School of Chemistry, Tel Aviv University, Tel Aviv 69978, Israel

hopping rates (see below). For different glassy electrolytes a_{eff} either increases or decreases with T (in the temperature ranges studied a linear behavior was observed). It was also found that $\sigma_3 > 0$, while σ_5 has different sign for different glass compositions. In the frequency-dependent response the real part $j'_3(\omega)$ of the third order harmonics $\hat{j}_3(\omega)$ has a negative sign for low frequency. With increasing frequency, $j'_3(\omega)$ increases and becomes positive close to the onset frequency of the dispersive part in the first order harmonics $j'_1(\omega)$ (which gives the linear response conductivity $\sigma'_3(\omega)$).

Taking disorder averages²² of the analytical expression for the current derived in ref. 18, it was suggested that the large values of a_{eff} have their origin in the spatial variation of hopping rates in the glassy material. Moreover, based on a small u expansion, it was predicted that $a_{\text{eff}} \propto M^{1/2}$, where $M \simeq L/a$ is the number of sites of the film sample in field direction. However, this result followed from the analytical result for the current by expanding terms such as $\exp(Mu)$ in powers of Mu . However, in the experimental studies on the nonlinear current response in glassy thin film electrolytes, values of Mu are always much larger than one and in such situation one should take the thermodynamic limit $M \rightarrow \infty$ before carrying out the small u expansion of the current.²⁶ This can lead to non-analyticities in the current response. It was argued²³ that these non-analyticities could spoil the analysis of nonlinear conductivities based on odd powers in the field amplitude, as they are commonly employed in experiments.

An open question is whether the rectification effects occurring in finite systems are present also in the thermodynamic limit. Intuitively, one would expect that in the absence of long-range correlations in the energy landscape (*i.e.* correlations decaying faster than $1/\text{distance}$), self-averaging effects will lead to larger reduction of rectification for larger system size. As a consequence one would predict rectification effects to disappear in the thermodynamic limit. While this is in agreement with experimental observations (for sample thicknesses so far studied), it has not yet been demonstrated by theoretical analysis. To avoid the problem of possible rectification effects and to enforce that the current is an odd function of u , energy landscapes with point symmetry were considered in ref. 22 and 23. However, the constraint of point symmetry implicitly introduces long-range correlations in the energy landscape and it is questionable if such procedure is suitable to describe real experimental situations.

In this work we treat the following open problems:

(1) Analytical results for the stationary current in ring system with M sites were derived up to now for the coupling $\propto \exp(\pm u/2)$ of the external bias $u = qEa/k_B T$ to the bare rates (rates in the absence of the external driving). This rate emerges naturally when approaching the hopping limit of the overdamped Brownian dynamics (Smoluchowski equation) of noninteracting particles. However, in interacting many-particle systems more complicated couplings of the rates to the external field can be imagined, when mapping the dynamics to an effective one-particle hopping process in a renormalized energy landscape. We therefore derive the stationary current for arbitrary couplings, and discuss in more detail the behavior for jump rates obeying the condition of detailed balance. We

find that is then possible to obtain already in an ordered system effective length scales a_{eff} significantly larger than the jump length a . Hence it appears that not only the disorder affects a_{eff} .

(2) As outlined above, for relating the theoretical results to experiments in the nonlinear regime, one should first perform the thermodynamic limit $M \rightarrow \infty$ before expanding the current in powers of the field amplitude. By performing this limit we also clarify the role of rectification effects for large M .

(3) For ring systems it is unclear how the periodic boundary conditions affect the stationary current. We therefore study the analogous problem in an open channel, where particles are injected and ejected from two particle reservoirs on the left and right side with electrochemical potentials μ_L and μ_R , respectively. The rates for the local exchange of particles with the reservoirs fulfil detailed balance with respect to the grand-canonical ensembles associated with μ_L and μ_R . We will treat the linear limit of the rate equations in this work to avoid boundary induced phase transitions as occurring in ASEPs or TASEPs.¹⁰⁻¹²

(4) Up to now the time-dependent nonlinear current response has been rarely studied.²⁷ Here we will investigate, for both the ring systems and open channels, this time-dependent response to a sinusoidal driving force with a large field amplitude E_0 by numerically solving the corresponding rate equations for the occupation probabilities. The data are analyzed by standard Fourier analysis in terms of harmonics $\hat{j}_n(\omega)$ of n th order. We present results for spatially uncorrelated barrier energies with uniform distributions and discuss the relation of the harmonics in the ring and open channel with respect to different frequency regimes.

2. Transition rates and energetic disorder

For convenient notation, we define $k_B T$ as the energy unit in the following, $k_B T = 1$. In a disordered energy landscape with site energies ε_k and energy barriers $U_{k,k+1} = U_{k+1,k}$ between sites k and $k + 1$, the rates $\Gamma_k^+(t)$ and $\Gamma_{k+1}^-(t)$ are considered to be functions of ε_k , ε_{k+1} , and $U_{k,k+1}$. In addition they depend on the external bias u , which we assume to be homogenous over the ring or channel, corresponding to a linear decrease of the external potential. If the rates obey detailed balance at each time instant, their ratio $\eta_k(t)$ is given by

$$\eta_k(t) = \frac{\Gamma_k^+(t)}{\Gamma_{k+1}^-(t)} = \exp(-\Delta E_{k,k+1}), \quad (1)$$

where

$$\Delta E_{k,k+1} = \varepsilon_{k+1} - \varepsilon_k - u. \quad (2)$$

In the presence of screening effects, the potential gradient is not constant, *i.e.* $\Delta E_{k,k+1}$ depends on k . The analytical formulae derived in the following sections can be generalized to this situation.

To illustrate our findings we will consider two types of rates and two types of energetic disorder. For the rates we use either the ‘‘exponential rates’’

$$\Gamma_k^+ = \frac{\gamma}{2} \exp(-U_{k,k+1}) \exp(-\Delta E_{k,k+1}/2) \quad (3)$$

or the Glauber rates²⁸

$$\begin{aligned}\Gamma_k^+ &= \frac{\gamma}{2} \exp(-U_{k,k+1}) \left[1 + \tanh\left(\frac{\Delta E_{k,k+1}}{2}\right) \right] \\ &= \gamma \frac{\exp(-U_{k,k+1})}{1 + \exp(-\Delta E_{k,k+1})},\end{aligned}\quad (4)$$

where γ is a bare jump rate. For the energetic disorder, we consider either pure barrier disorder (all $\varepsilon_k = 0$), or pure site energy disorder (all barriers $U_{k,k+1} = 0$). The barrier and site energies are uncorrelated random variables drawn from box distributions, $U_{k,k+1} \in [0, \Delta_U]$ and $\varepsilon_i \in [-\Delta_\varepsilon/2, \Delta_\varepsilon/2]$ with widths Δ_U and Δ_ε , respectively.

3. Conduction in ring systems

We study the nearest neighbor hopping of one particle on a ring with M sites $i = 1, \dots, M$. The rates for a jump from site i backward and forward at time t are denoted as $\Gamma_i^-(t)$ and $\Gamma_i^+(t)$, respectively. The probabilities $p_i(t)$ for the particle to be on site i at time t obey the rate equations

$$\dot{p}_i = j_{i-1,i}(t) - j_{i,i+1}(t), \quad i = 1, \dots, M, \quad (5)$$

with the local currents

$$j_{i,i+1}(t) = \Gamma_i^+(t)p_i(t) - \Gamma_{i+1}^-(t)p_{i+1}(t), \quad i = 1, \dots, M. \quad (6)$$

In writing eqn (5) and (6) and further equations below we implicitly assume that the periodic boundary conditions are taken into account if the index i falls out of the range $1, \dots, M$, *i.e.* $p_{i+M}(t) = p_i(t)$, $\Gamma_{i+M}^\pm(t) = \Gamma_i^\pm(t)$, $j_{i+M,i+1+M}(t) = j_{i,i+1}(t)$, *etc.* The rate equations preserve the normalization $\sum_{i=1}^M p_i(t) = 1$.

Due to the normalization of the occupation probabilities to one particle, the current j refers to the single particle current. If we consider a total number N of non-interacting particles corresponding to a number density $n = N/M$ per lattice site, the total current is

$$J = Nj = nMj. \quad (7)$$

In the case of charged particles the corresponding charge current per lattice site is qJ and the charge current density qJ/A , where A is a cross sectional area associated with each lattice bond.

3.1 DC current

In a static (time-independent) driving field u the system reaches a stationary state at long times, where the occupation probabilities become constant, $p_i = p_i^{\text{st}}$, and all local currents in eqn (6) are equal, $j_{i,i+1} = j_{\text{dc}}$. Setting $\kappa_i = 1/\Gamma_{i+1}^-$ this leads to the recursion relation

$$p_{i+1}^{\text{st}} = \eta_i p_i^{\text{st}} - \kappa_i j_{\text{dc}}, \quad (8)$$

with solution

$$p_i^{\text{st}} = j_{\text{dc}} \frac{\sum_{k=1}^M \kappa_{i-k} \prod_{l=1}^{k-1} \eta_{i-l}}{\prod_{k=1}^M \eta_{i-k} - 1}. \quad (9)$$

The current j_{dc} follows from the normalization,

$$\frac{1}{j_{\text{dc}}} = \sum_{i=1}^M \frac{\sum_{k=1}^M \kappa_{i-k} \prod_{l=1}^{k-1} \eta_{i-l}}{\prod_{k=1}^M \eta_{i-k} - 1}, \quad (10)$$

which in turn fixes the occupation probabilities p_i^{st} . Eqn (9) and (10) hold true for arbitrary set of rates (as long as they do not exclude the formation of a unique stationary state).

For detailed balanced rates these expressions can be simplified. With condition (1) we have

$$\prod_{l=1}^k \eta_{i-l} = \exp(\varepsilon_{i-k} - \varepsilon_i + ku) \quad (11)$$

so that eqn (10) can be written in the form

$$\frac{1}{j_{\text{dc}}} = \frac{e^{-u/2}}{e^{Mu} - 1} \sum_{l=1}^M e^{lu} \sum_{k=1}^M \frac{\exp[(\varepsilon_k + \varepsilon_{k+1})/2]}{\sqrt{\Gamma_k^+(u)\Gamma_{k+1}^-(u)}} \exp(-\varepsilon_{k+1}), \quad (12)$$

where we explicitly indicated the dependence of the jump rates $\Gamma_k^\pm = \Gamma_k^\pm(u)$ on the external bias u . For the coupling $\propto \exp(\pm u/2)$ of the rates to the external field it can be shown that this formula agrees with eqn (10) in ref. 18 (or with eqn (8)–(11) in ref. 22).

In the linear response limit $u \rightarrow 0$, eqn (12) reduces to the result²⁹ $qJ_{\text{dc}}/A = qnMj/A = \sigma_1 E_0$ with

$$\sigma_1 = \frac{nq^2 a^2}{k_B T} \left(\frac{1}{M} \sum_{k=1}^M \frac{1}{p_k^{\text{eq}} \Gamma_k^+} \right)^{-1}, \quad (13)$$

where $p_k^{\text{eq}} \propto \exp(-\varepsilon_k)$ is the equilibrium distribution and Γ_k^\pm are the rates in the absence of external driving ($u = 0$). This formula can be viewed as resulting from the combination in series of conductances $\propto p_k^{\text{eq}} \Gamma_k^+$.

In systems with only barrier disorder (all sites have the same energy $\varepsilon_k = 0$), eqn (12) reduces to

$$\frac{1}{j_{\text{dc}}} = \frac{1}{2 \sinh(u/2)} \sum_{k=1}^M \frac{1}{\sqrt{\Gamma_k^+(u)\Gamma_{k+1}^-(u)}}. \quad (14)$$

Because $\Gamma_k^+(-u) = \Gamma_{k+1}^-(u)$ in this case, we have $\Gamma_k^+(-u)\Gamma_{k+1}^-(u) = \Gamma_{k+1}^-(u)\Gamma_k^+(u) = \Gamma_k^+(u)\Gamma_{k+1}^-(u)$, and it follows that $j(-u) = -j(u)$ for each disorder configuration. This is at first sight a surprising result, since one could consider an asymmetric spatial arrangement of barriers, for example, $U_{k,k+1} = kU_0$ for $k = 1, \dots, M$ and $U_0 > 0$. If a particle was driven in the direction of increasing k , it would encounter increasing barriers until a jump from the largest to the smallest barrier occurred (after passing the barrier $U_{M,M+1} = U_{M,1}$ between sites M and 1). When driving the particle in the reverse direction, the opposite behavior would result, *i.e.* the particle would encounter smaller and smaller barriers until a jump from the smallest barrier to the largest occurs.

Moreover, as long as the barriers for the local transitions are taken into account by a simple Boltzmann factor, *i.e.* $\Gamma_k^+(u) \propto \exp(-U_{k,k+1})f_+(u)$ and $\Gamma_{k+1}^-(u) \propto \exp(-U_{k,k+1})f_-(u)$ with functions $f_\pm(u)$ independent of k , one obtains the same current–voltage curve $J(u) = nMj(u)$ as in an ordered system up to a rescaling factor. In such ordered system,

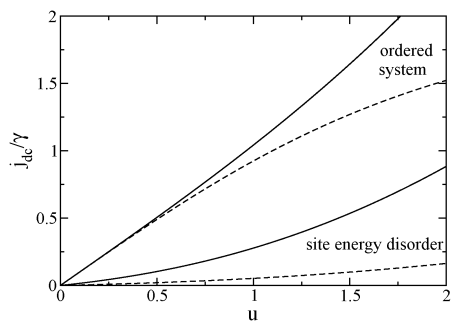


Fig. 1 Current $j_{dc}(u)$ in the ring system as a function of the bias u for the exponential rates (solid line) and the Glauber rates (dashed line). Results are shown for an ordered system and a box distribution of site energies with $\Delta_\epsilon = 6$. In the system with site energy disorder the mean current is shown, obtained after averaging j_{dc} from eqn (10) over 100 realizations. In the case of pure barrier disorder the same curves as in the ordered system are obtained for each disorder realization up to a (realization-dependent) rescaling of the current (see text).

$\Gamma_k^+ \Gamma_{k+1}^- = \Gamma^+ \Gamma^-$ is independent of k , and one obtains an M independent total current $J_{dc} = nMj_{dc}$,

$$J_{dc}(u) = 2n \sinh\left(\frac{u}{2}\right) \sqrt{\Gamma^+(u)\Gamma^-(u)}. \quad (15)$$

Fig. 1 shows the current $J_{dc}(u)$ in the ordered ring system (or in the ring systems with barrier disorder) for the exponential rates (3) and the Glauber rates (4). For comparison we also show the average current $J_{dc}(u)$ in the case of the box distribution of site energies with $\Delta_\epsilon = 6$. The current was calculated according to eqn (7) and (12) and averaged over 10^3 different realizations of the site energy disorder in rings with $M = 10^3$ sites. The current-voltage curves in the experimentally relevant regime $u \lesssim 1$ tend to have a more convex shape in the presence of site energy disorder. For the Glauber rates the current is smaller and saturates for $u \rightarrow \pm\infty$.

In the ordered ring system, for the generic coupling $\Gamma^\pm(u) = (\gamma/2)\exp(\pm u/2)$, one recovers from eqn (15) the known result for the charge current density²⁵

$$\frac{qJ_{dc}}{A} = \frac{\gamma qn}{A} \sinh\left(\frac{u}{2}\right) = \sigma_1 E + \sigma_3 E^3 + \mathcal{O}(E^5) \quad (16)$$

with $\sigma_1 = (n/aA)\gamma q^2 a^2 / 2k_B T$ and $\sigma_3 = (n/aA)\gamma q^4 a^4 / 48(k_B T)^3$. These results motivate to define an effective jump length by

$$a_{\text{eff}}^2 = \frac{24(k_B T)^2 \sigma_3}{q^2 \sigma_1}. \quad (17)$$

However, even in an ordered system it is possible that this effective jump length does not yield a reasonable estimate of the true jump length a . The reason is that, while the linear response quantity σ_1 is universal (*i.e.* independent of the specific form of the jump rates), this is not the case for the nonlinear conductivity σ_3 . For example, for the Glauber rates, we obtain $J = \gamma n \tanh(u/2)$ from eqn (15) and accordingly a negative $\sigma_3 = -(n/aA)\gamma q^4 a^4 / 24(k_B T)^3$. If this would be inserted in eqn (17), a_{eff} became imaginary.

In the general case, we can expand $\Gamma^+(u)$ in a Taylor series, $\Gamma^+(u) = (\gamma/2)(1 + \alpha_1 u + \alpha_2 u^2 + \alpha_3 u^3 + \dots)$. From $\Gamma^-(u) = \Gamma^+(-u) = \exp(-u)\Gamma^+(u)$ it follows that $\alpha_1 = 1/2$ independent

of the specific form. With eqn (15) we find $\sigma_3/\sigma_1 = (\alpha_2 - 1/12)q^2 a^2 / (k_B T)^2$, *i.e.*

$$a_{\text{eff}}^2 = 24\left(\alpha_2 - \frac{1}{12}\right)a^2. \quad (18)$$

We conclude that depending on α_2 different a_{eff} can be obtained even in an ordered system. For example, we obtain $\alpha_2 = 1/8$ for the exponential rates, yielding $a_{\text{eff}} = a$, while for the Glauber rates we obtain $\alpha_2 = 0$, yielding $a_{\text{eff}}^2 = -2a^2$.

3.2 Thermodynamic limit and rectification

In the thermodynamic limit $M \rightarrow \infty$ the sum over k in eqn (12) can be replaced by a disorder average $\langle \dots \rangle$ if the site energies and energy barrier do not exhibit very broad distributions or long-range correlations, *i.e.* if the system is self-averaging. Accordingly we define

$$a_l(u) = \lim_{M \rightarrow \infty} \frac{1}{M} \sum_{k=1}^M \frac{\exp[(\epsilon_k + \epsilon_{k+1})/2]}{\sqrt{\Gamma_k^+(u)\Gamma_{k+1}^-(u)}} \exp(-\epsilon_{k+l})$$

$$= \begin{cases} \left\langle \frac{\exp[(\epsilon_1 - \epsilon_2)/2]}{\sqrt{\Gamma^+(u; U_{12}, \epsilon_1, \epsilon_2)\Gamma^-(u; U_{12}, \epsilon_1, \epsilon_2)}} \right\rangle, \\ \left\langle \frac{\exp[(\epsilon_1 + \epsilon_2)/2] \exp(-\epsilon_3)}{\sqrt{\Gamma^+(u; U_{12}, \epsilon_1, \epsilon_2)\Gamma^-(u; U_{12}, \epsilon_1, \epsilon_2)}} \right\rangle, \\ \left\langle \frac{\exp[(\epsilon_2 - \epsilon_1)/2]}{\sqrt{\Gamma^+(u; U_{12}, \epsilon_1, \epsilon_2)\Gamma^-(u; U_{12}, \epsilon_1, \epsilon_2)}} \right\rangle, \end{cases} \quad (19)$$

where the first and third case in the last line refer to $l = 1$ and $l = M$, respectively, and the second case to $l = 2, \dots, M-1$; we took into account the periodic boundary conditions and have explicitly denoted the dependence of the jump rates $\Gamma_k^\pm(u) = \Gamma^\pm(u; U_{k,k+1}, \epsilon_k, \epsilon_{k+1})$ on the energies.

Keeping the number density n fixed in the limit $M \rightarrow \infty$, we then obtain from eqn (12) for the total current

$$J_{dc}(u) = 2n \sinh\left(\frac{u}{2}\right) \times \frac{e^{|u|}}{[\theta(-u)a_1(u) + \theta(u)a_M(u)](e^{|u|} - 1) + a_2(u)}, \quad (20)$$

where $\theta(\cdot)$ is the Heaviside step function [$\theta(x) = 1$ for $x \geq 0$, and zero else]. As discussed in the Introduction, the thermodynamic limit should apply to typical experiments on thin film electrolytes and there should be no notable dependence of the current (and the nonlinear conductivities) on the film thickness, in agreement with the experimental observations. However, the one-dimensional treatment of two- or three-dimensional geometries (as, *e.g.*, thin film electrolytes) requires a mean-field treatment, where the concentrations represent averages over a larger number of sites belonging to lines or planes perpendicular to the current direction. Hence, it is possible that fluctuation effects induced by hops in directions perpendicular to the field, can destroy the non-analyticities predicted by eqn (20). The role of such fluctuations is not clear at present and needs further investigation.

We can further show that the current from eqn (20) is antisymmetric with respect to the bias u . To this end we have

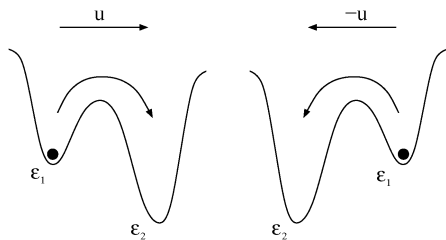


Fig. 2 Two mirror configurations with interchanged site energies ε_1 and ε_2 (and same ε_3 , not shown), as appearing with equal statistical weight in the averages in eqn (19). The jump rate $\Gamma^+(u; U_{12}, \varepsilon_1, \varepsilon_2)$ in the left configuration is equal to the jump rate $\Gamma^-(-u; U_{12}, \varepsilon_2, \varepsilon_1)$ in the right configuration after reversal of the bias u .

to analyze the symmetry properties of the $a(u)$. Note that in the averages in eqn (19) there occur configurations with two or three sites only, having mutually independent random site energies $\varepsilon_1, \dots, \varepsilon_3$. As illustrated in Fig. 2, to each realization of the two energies ε_1 and ε_2 there exists a “mirror configuration” with interchanged site energies ε_1 and ε_2 , and the same value of ε_3 . Since these mirror configurations occur with equal statistical weight and exhibit the symmetry property $\Gamma^+(u; U_{12}, \varepsilon_1, \varepsilon_2) = \Gamma^-(-u; U_{12}, \varepsilon_2, \varepsilon_1)$, we can use $\Gamma^+(u; U_{12}, \varepsilon_1, \varepsilon_2) \Gamma^-(-u; U_{12}, \varepsilon_1, \varepsilon_2) = \Gamma^+(-u; U_{12}, \varepsilon_2, \varepsilon_1) \Gamma^-(-u; U_{12}, \varepsilon_2, \varepsilon_1)$ in the averages of eqn (19). This implies $a_1(-u) = a_M(u)$ and $a_2(-u) = a_2(u)$, leading to $J(-u) = -J(u)$. Let us note that this does not imply that the expansion of $J(u)$ contains odd powers of u only. Terms $\propto |u|^{2n+1}u$, $n = 0, 1, \dots$, can occur according to eqn (20) (see also the discussion in ref. 23 for the consequences of these non-analytic terms with respect to the analysis of experiments).

In view of the antisymmetric property of the current in the thermodynamic limit, we expect that, due to self-averaging, rectification effects for each configuration of the disorder will become smaller with increasing system size. To check this expectation, we define the rectification parameter

$$R(u, M) = \frac{J_{\text{dc}}(u) + J_{\text{dc}}(-u)}{J_{\text{dc}}(u) - J_{\text{dc}}(-u)} \quad (21)$$

for each disordered configuration in a ring with M sites with $J_{\text{dc}}(u) = nMj$ and j_{dc} from eqn (10). The distribution of this rectification parameter is, on symmetry reasons, an even function of u , hence $\langle R(u, M) \rangle = 0$. In the case of

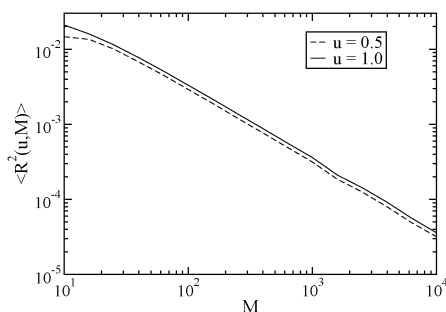


Fig. 3 Variance $\langle R^2(u, M) \rangle$ of the distribution of the rectification parameter $R(u, M)$ for the ring system in dependence of the system size M at two fixed values of the bias u . The $R(u, M)$ were calculated from eqn (12),(23) for a box distribution of site energies with $\Delta_\varepsilon = 6$ and disorder averages were performed over 10^3 – 10^5 realizations.

self-averaging, the variance $\langle R(u, M)^2 \rangle$ should decrease as $\sim 1/M$ for $M \rightarrow \infty$. As shown in Fig. 3, this behavior is nicely confirmed by taking disorder averages of $R^2(u, M)$.

4. Conduction in open channels

So far we have considered ring systems with periodic boundary conditions. In many situations the coupling of the system to particle reservoirs is of importance, as in molecular wires, membrane ion channels, and thin-film electrolytes in contact with non-blocking electrodes. In these systems details of the contact with the reservoir can play a decisive role for the transport behavior, so that a specific treatment is needed for the particular system under consideration.

On the other hand, to elucidate the generic features of the particle transport, it is sufficient to adopt a coarse-grained description, where only a few external parameters enter, as, for example, the thermodynamic driving force that brings the system into equilibrium with itself. Based on such a coarse-grained description we will, in the following, characterize a reservoir by its chemical potential (corresponding to a “site energy level” relative to the site energies of the system), and by the energy barrier for exchanging particles between it and the system.

To be specific, we consider a one-dimensional channel consisting of M sites, which is coupled to sites $k = 0$ and $k = M + 1$, belonging to two reservoirs with chemical potentials $\mu_L^0 = \varepsilon_0$ and $\mu_R^0 = \varepsilon_{M+1}$, respectively. Particles are injected or ejected from the two reservoir sites with rates that fulfil the condition of detailed balance with respect to the grand-canonical ensembles associated with μ_L^0 and μ_R^0 . As for the ring system, the site energies ε_k and the barrier energies $U_{k,k+1}$, $k = 0, \dots, M$, determine the jump rates in the absence of the external bias u , see section 2 ($U_{0,1}$ and $U_{M,M+1}$ specify the energy barriers for exchange of particles with the left and right reservoir, respectively). In the presence of a spatially uniform bias u , the potential drop along the channel leads to the site energies

$$E_k = \varepsilon_k - ku, \quad (22)$$

and the electrochemical potentials

$$\mu_L = E_0 = \mu_L^0 \text{ and } \mu_R = E_{M+1} = \mu_R^0 - (M + 1)u, \quad (23)$$

if we locate the point of zero external potential at the left end of the channel. Note that for $k = 0$ and $k = M$, eqn (1),(3),(4) define the jump rates for entering and leaving the system, in agreement with detailed balance with respect to the grand-canonical ensembles associated with $\mu_L^0 = \varepsilon_0$ and $\mu_R^0 = \varepsilon_{M+1}$.

In the open channel the particle number is a random variable and it is not possible to consider a single-particle approach from the beginning. The rate equations for the local concentrations $p_i = \langle n_i \rangle$ follow from a Fermi lattice gas model, where the occupation numbers n_i at each site can have only two values $n_i = 0$ (vacant site) or $n_i = 1$ (occupied site), and the set $\{n_i\}$ specifies the microstate in the channel. The average $\langle \dots \rangle$ has to be taken with respect to the probability distribution of the microstates at time t , whose time evolution follows a master equation. Based on the master equation, the derivation of the currents $j_{i,i+1}$ in the equations of motions

(5) is straightforward (for a systematic approach, including also models with particle–particle interactions going beyond site exclusion, see ref. 30). The result is

$$j_{i,i+1} = \Gamma_i^+ \langle n_i(1 - n_{i+1}) \rangle - \Gamma_{i+1}^- \langle n_{i+1}(1 - n_i) \rangle \quad (24)$$

for $i = 1, \dots, M - 1$. For the boundary currents specifying the exchange of particles with the reservoirs one obtains

$$j_{0,1} = \Gamma_0^+ (1 - p_1) - \Gamma_1^- p_1, \quad (25a)$$

$$j_{M,M+1} = \Gamma_M^+ p_M - \Gamma_{M+1}^- (1 - p_M). \quad (25b)$$

In a mean-field approximation, $\langle n_i n_{i+1} \rangle \simeq \langle n_i \rangle \langle n_{i+1} \rangle = p_i p_{i+1}$, the currents in eqn (24) can be expressed as

$$j_{i,i+1} = \Gamma_i^+ p_i (1 - p_{i+1}) - \Gamma_{i+1}^- p_{i+1} (1 - p_i) \quad (26)$$

for $i = 1, \dots, M - 1$. In contrast to the ring system, the p_k are no longer normalized (the total population is not conserved), but the mean number density \bar{p} of particles is, for fixed energy disorder, controlled by the electrochemical potentials μ_L and μ_R . Accordingly, the currents $j_{i,i+1}$ in eqn (26) and (25) are particle currents (rather than probability currents) along the bonds between sites i and $i + 1$.

The nonlinear dependence on the p_i leads, for non-vanishing bias $u > 0$, to interesting phase transitions of the mean particle density with respect to variations of μ_L and μ_R , even in systems without energetic disorder.³¹ Based on exact solutions of the nonlinear mean-field rate equations, one can show that these phase diagrams are correctly predicted by the mean-field approximation.³² The fact that phase transitions can occur also in the dilute limit is sometimes disregarded. For example, it has not been considered in treatments of incoherent hopping transport of electrons in molecular wires, *e.g.* along DNA molecules.

A thorough study of the nonlinear eqn (26) in the presence of energetic disorder goes beyond the scope of this work. In the special case of pure barrier disorder (all $\varepsilon_i = 0$) and a current driven solely by a chemical potential difference $\Delta\mu_0 = \mu_L^0 - \mu_R^0$ (bulk bias $u = 0$), one has $\Gamma_i^+ = \Gamma_{i+1}^-$, and the nonlinear terms $\propto p_i p_{i+1}$ in eqn (26) cancel. Accordingly, an analytical solution of eqn (25),(26) can be obtained for the stationary state following the procedure discussed in the following section 4.1. The result for the corresponding dc-current reads

$$J_{\text{dc}} = \frac{\Gamma_0^+ (\Gamma_M^+ + \Gamma_{M+1}^-) - \Gamma_{M+1}^- (\Gamma_0^+ + \Gamma_1^-)}{(\Gamma_0^+ + \Gamma_1^-) + (\Gamma_M^+ + \Gamma_{M+1}^-) \left[1 + (\Gamma_0^+ + \Gamma_1^-) \sum_{l=1}^{M-1} \frac{1}{\Gamma_l^+} \right]}. \quad (27)$$

Note that due to the physical meaning of the $j_{i,i+1}$ discussed above, the (total) current J_{dc} appears in eqn (27).

In what follows we will focus on situations where the consideration of the one-dimensional geometry is an approximation for a preferred bias direction of a higher-dimensional system, *i.e.* the p_i in eqn (25),(26) are mean concentrations (per site) that represent averages over a larger number of sites belonging to lines or planes perpendicular to the current direction. In this case we can, without worrying about the boundary-induced phase transitions in one-dimensional

geometries, consider the dilute limit of eqn (26) with $1 - p_i \simeq 1$,

$$j_{i,i+1} = \Gamma_i^+ p_i - \Gamma_{i+1}^- p_{i+1}, \quad i = 1, \dots, M - 1. \quad (28)$$

The rate equations for the occupation probabilities $p_i(t)$ now have the same form as in eqn (5) for the single-particle transport on the ring, but we have to take into account the boundary currents according to eqn (25). Moreover, one should keep in mind that the p_i , according to the derivation of eqn (26), should be much smaller than one.³³

In total five external parameters control the transport behavior in our model for the open channel: the chemical potentials μ_L^0 and μ_R^0 ; the energy barriers $U_{0,1}$ and $U_{M,M+1}$ for particle exchange of the system with the reservoirs; and the bias u . In the following, we will in most cases consider the μ_L^0 , μ_R^0 , $U_{0,1}$, $U_{M,M+1}$ to be given and discuss the transport behavior with respect to the bias u .

4.1 DC current

To calculate the stationary current under a static bias we iterate eqn (8) to obtain

$$p_k^{\text{st}} = A_{k-1} p_1^{\text{st}} - J_{\text{dc}} B_{k-1}, \quad (29)$$

with

$$A_k = \prod_{l=1}^k \eta_l = \exp[(E_1 - E_{k+1})], \quad (30)$$

$$B_k = \sum_{m=1}^k \kappa_m \prod_{l=m+1}^k \eta_l = \sum_{m=1}^k \kappa_m \exp(E_{m+1} - E_{k+1}), \quad (31)$$

where the expression containing the products hold true in general, while the second expressions are valid for detailed balanced rates.

Using eqn (25) together with eqn (29) for $k = M$ one obtains a closed equation for J_{dc} with solution

$$J_{\text{dc}} = \frac{1 - \exp[-(\mu_L^0 - \mu_R^0) - (M + 1)u]}{\frac{1}{\Gamma_0^+} + \frac{\exp[-\varepsilon_M - Mu - \mu_L^0]}{\Gamma_M^+} + \sum_{k=1}^{M-1} \frac{\exp(\varepsilon_k - \mu_L^0 - ku)}{\Gamma_k^+}} \quad (32a)$$

$$= \frac{1 - \exp(-\Delta\mu)}{\sum_{k=0}^M (\Gamma_k^+)^{-1} \exp(E_k - \mu_L)}, \quad (32b)$$

where $\Delta\mu = \Delta\mu_0 - (M + 1)u$. This result in turn determines the local concentrations p_k^{st} in eqn (29) *via* eqn (30),(31) and p_1^{st} from eqn (25a) with $j_{0,1} = J_{\text{dc}}$.

Eqn (32b) may be interpreted in a similar way as the linear response in the ring system, *cf.* eqn (13): The current follows from a driving force $1 - \exp(-\Delta\mu)$ and a total “conductance” is given by combining elementary “conductances” $\exp[-(E_k - \mu_L)] \Gamma_k^+$ in serial order. Eqn (32b) is, however, not a linear response formula, but describes the full nonlinear response to the bulk driving force u and the boundary driving force $\Delta\mu_0$. Note that these driving forces do not enter eqn (32b) in the single combination $\Delta\mu = \Delta\mu_0 - (M + 1)u$, since Γ_0^+ and Γ_M^+ are controlled independently by μ_L^0 and μ_R^0 , respectively.

Due to the factors $\propto \exp(-ku)$ in eqn (32b), only jump rates Γ_k^+ (Γ_{M-k}^+), $k = 1, 2, \dots$, from sites close to the left (right) boundary give a significant contribution for positive (negative) bias u . This means that for $u \neq 0$, J_{dc} is governed by jump rates belonging to sites in a region of size $\propto 1/u$ close to either boundary. As a consequence, already pure barrier disorder (with all $\varepsilon_k = 0$) leads to rectification effects in the open channel, in marked contrast to the behavior in the ring system.

It may be surprising at first sight that the dominant contribution to the current comes from regions close to either boundary (for similar phenomena expected in connection with electron transport through molecular bridges, see ref. 34). The effect can be understood when considering, without generality, $u > 0$, and a single large barrier $U_{l,l+1} > U_0$ in an otherwise ordered system with smaller barriers $U_{k,k+1} = U_0$ for $k \neq l$ (and all $\varepsilon_k = 0$). Let us first look at the density profile in the region of sites left [$k \leq l$] and right [$k \geq (l+1)$] of the large barrier. For the current $j_{l,l+1} > 0$ across the large barrier $U_{l,l+1}$ to equal all other currents $j_{k,k+1}$, the concentrations in the left region “before the large barrier” have to be much larger than in the right region “after the large barrier”. The higher concentration before the large barrier influences the

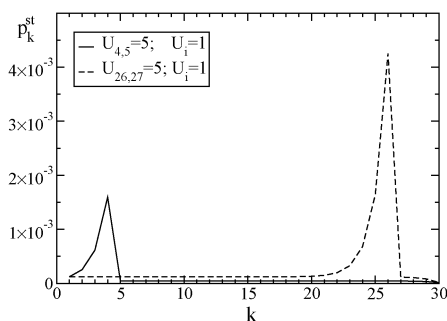


Fig. 4 Stationary density profiles in an open channel with $M = 30$ sites, a constant bias $u = 1$ and a single large barrier $U_{l,l+1} = 5$ close to the left ($l = 4$, solid line) and close to the right boundary ($l = 26$, dashed line); the other barriers are set to one, $U_{k,k+1} = 1$ for $k \neq l$ (including the boundary barriers for exchange of particles with the reservoirs with $\mu_{\text{R}}^0 = \mu_{\text{L}}^0 = -10$) and all $\varepsilon_k = 0$, $k = 0, \dots, M+1$. As a consequence of the density profile, the current $J = 1.8 \times 10^{-5}$ for the large barrier at site $l = 4$ is smaller than the current $J = 4.7 \times 10^{-5}$ for the larger barrier at site $l = 26$. In the latter case J has practically the same value as in the corresponding ordered system (all $U_{k,k+1} = 1$).

value p_1^{st} right of the left boundary with a strength decreasing with increasing distance from the large barrier (smaller k). The value p_1^{st} in turn determines the current $\Gamma_0^+ - \Gamma_1^- p_1^{\text{st}} = j_{\text{st}}$. More generally speaking, we can say that for $u > 0$ ($u < 0$) the energy landscape close to the left (right) boundary controls the density at the boundary site $k = 1$ ($k = M$) and thus the current $J_{\text{dc}} = j_{0,1}$ ($J_{\text{dc}} = j_{M,M+1}$). The effect is demonstrated in Fig. 4, where we show the solution p_k^{st} for a large barrier close to the left boundary (solid line) and close to the right boundary (dashed line). As a consequence, when the large barrier is closer to the left boundary, the density at the boundary site $k = 1$ becomes larger, leading to a smaller current $J_{\text{dc}} = j_{0,1}$. We note that the dominance of the boundary regions will no longer apply when considering the transport with site exclusion in strictly one-dimensional topologies (ASEPs or TASEPs).

To illustrate typical current behavior, we calculate J_{dc} as a function of the driving forces for only barrier disorder (all $\varepsilon_k = 0$) and for only site energy disorder (all $U_{k,k+1} = 0$), using the box distributions introduced in section 2. Fig. 5 shows results for the disorder averaged current (a) as a function of u for $\mu_{\text{L}}^0 = \mu_{\text{R}}^0 = -10$, and (b) as a function of $\Delta\mu_0$ for $\mu^0 = -10$ ($\mu_{\text{L,R}}^0 = -10 \pm \Delta\mu_0$) and $u = 0$. Similarly to the ring system, the current–voltage curves in Fig. 5a have a more convex shape in the presence of site energy disorder for small u . One may ask if the current $j_{\text{dc}}^{\text{ring}}$ in the ring system [eqn (12)] and the current $J_{\text{dc}}^{\text{ch}}$ in the open channel [eqn (32)] can be connected by simply taking into account the mean number $\bar{N} = \sum_k^M =_1 p_k^{\text{st}}$ of particles in the channel, *i.e.* if $J_{\text{dc}}^{\text{ch}} = \bar{N} J_{\text{dc}}^{\text{ring}}$. However, the fact that regions close to either boundary govern the value of $J_{\text{dc}}^{\text{ch}}$, already shows that such mapping cannot be correct. Indeed, based on the analytical results^{12,35} obtained for the ring system and open channel, one can show that such a relation does not hold true. Numerical solutions also show that the relation does not provide a reasonable approximation (see also the discussion in section 5).

4.2 Thermodynamic limit and rectification

The dominance of the boundary regions implies that the thermodynamic limit has to be taken in such a way that for $u > 0$ the left boundary has to be fixed and the right boundary goes to infinity, while for $u < 0$ one should consider the reversed situation (fixed right boundary and left boundary

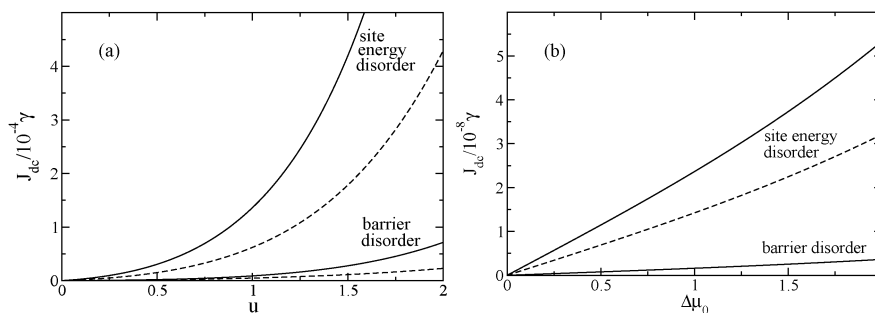


Fig. 5 Current J_{dc} (a) as a function of the bias u at fixed $\mu_{\text{L}}^0 = \mu_{\text{R}}^0 = -10$ and (b) as a function of the chemical potential difference $\Delta\mu_0$ for vanishing bias $u = 0$. Averages have been performed over 100 realizations of the disorder, for a box distribution of energy barriers with $\Delta_U = 5$ and a box distribution of site energies with $\Delta_\varepsilon = 6$. Solid lines refer to the exponential rates and dashed lines to the Glauber rates. In the case of barrier disorder and $u = 0$, the exponential and Glauber jump rates are the same and hence the corresponding currents agree in part (b).

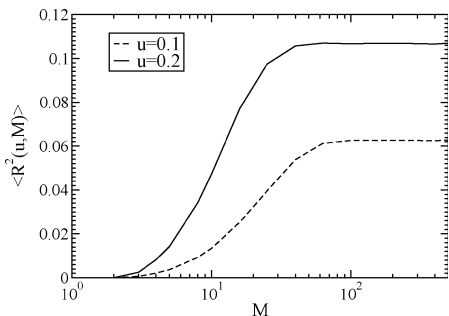


Fig. 6 Variance $\langle R^2(u, M) \rangle$ of the distribution of the rectification parameter $R(u, M)$ for the open channel in dependence of the system size M at two fixed values of the bias u . The $R(u, M)$ were calculated from eqn (32),(21) for a box distribution of site energies with $\Delta_\varepsilon = 6$ and disorder averages were performed over 10^3 – 10^5 realizations.

going to infinity). We focus on the case $u > 0$ here (with obvious analogous treatment for the case $u < 0$). For $M \rightarrow \infty$, eqn (32b) then becomes

$$J_{\text{dc}} = \frac{1}{\sum_{k=0}^{\infty} (\Gamma_k^+)^{-1} \exp(E_k - \mu_L)}. \quad (33)$$

One can prove that in the special case of point-symmetric energy landscapes ($\varepsilon_k = \varepsilon_{M+1-k}$, $U_{k,k+1} = U_{M+1-k, M-k}$) the current is antisymmetric with respect to a reversal of the driving forces, i.e. $J_{\text{dc}}(-u, \mu_L \rightarrow \mu_R, \mu_R \rightarrow \mu_L) = -J(u, \mu_L, \mu_R)$ (the reference point of zero external potential has to be shifted from the left to right boundary also).

On the hand, in general rectification effects occur already for pure barrier disorder and do not become smaller for increasing M . Accordingly, the width of the distribution of the rectification parameter defined in eqn (21) should saturate to a finite value for $M \rightarrow \infty$. This is confirmed in Fig. 6, where for pure energy disorder, $\langle R^2(u, M) \rangle$ is shown as a function of M for two fixed values of u and $\mu_L^0 = \mu_R^0 = -10$. It would be interesting to check this theoretical prediction in experiments, e.g. in thin film electrolytes contacted to non-blocking electrodes. Systematic measurements in dependence of the system size (film thickness) would allow one to distinguish between a possible finite size effect and the effects induced by the open boundaries.

5. Time-dependent nonlinear response

In this section we discuss the time-dependent nonlinear response to a sinusoidal electric field $E(t) = E_0 \sin(\omega t)$ with large amplitude E_0 , corresponding to a bias $u(t) = u_0 \sin(\omega t)$ with amplitude $u_0 = qE_0 a / k_B T \gtrsim 1$. To this end we solve the rate eqn (5) supplemented by periodic boundary conditions for the ring and eqn (25) for the open channel. After a transient time interval the stationary regime is reached, where we determine the total current $J_{\text{st}}(t)$ averaged over many periods. Fourier decomposition of this stationary current yields the complex first order and higher harmonics $\hat{J}_n(\omega) = J_n'(\omega) + iJ_n''(\omega)$, $n = 1, 2, \dots$

In the zero and infinite frequency limit, the current $J_{\text{st}}(t)$ (and hence the harmonics $\hat{J}_n(\omega)$) can be calculated analytically.

For $\omega \rightarrow \infty$ and barrier disorder, the mean local densities $p_i(t)$ in the stationary state become independent of position and time, i.e. $p_i(t) = p_i^{35}$ and one can show that for each realization

$$J_{\text{st}}(t) = \frac{\gamma p}{2M} \left[\sum_{k=1}^M \exp(-U_{k,k+1}) \right] [f_+(u(t)) - f_-(u(t))], \quad (34)$$

where $f_{\pm}(u)$ are the factors modifying the transitions due to the external driving [see discussion above eqn (15)]. Upon averaging over the disorder (or due to self-averaging), $\sum_{k=1}^M \exp(-U_{k,k+1}) / M$ can be replaced by the ensemble average $\langle \exp(-U_{1,2}) \rangle$.

For $\omega = 0$, one can take the quasistatic limit,

$$J_{\text{st}}(t) = J_{\text{dc}}(u(t)) \quad (35)$$

with $J_{\text{dc}}(\cdot)$ from eqn (12) for the ring system and eqn (32) for the open channel. For exploring the intermediate frequency behavior we have to rely on our numerical solution of the underlying rate equations.

In the following we will focus on the barrier disorder case, implying that harmonics of even order vanish in the ring due to the absence of rectification (see the discussion in section 3.2). In the open channel, by contrast, rectification effects are present and the harmonics of even order are nonzero. However, these harmonics of even order are much smaller than the harmonics of odd order, and therefore will not be shown here. For the discussion of the harmonics of odd order we focus on the real parts $J_3'(\omega)$.

Fig. 7 shows the harmonics $J_1'(\omega)$ and $J_3'(\omega)$ in the case of the exponential jump rates for the barrier disorder with $\Delta U = 2$ and bias amplitude $u_0 = 1$ (for the channel we have set $\mu_L^0 = \mu_R^0 = -1$ and boundary barriers $U_{0,1} = U_{M,M+1} = 2.2$). The results were averaged over 5 realization of the disorder. The circles mark the results for the ring system and the squares for the open channel.

In the ring system, the first harmonic $J_1'(\omega)$ shows the typical behavior known for a hopping system in the linear response limit: In a high frequency regime, $J_1'(\omega)$ shows a plateau, and then, upon lowering the frequency, it decreases monotonously within a dispersive regime until approaching

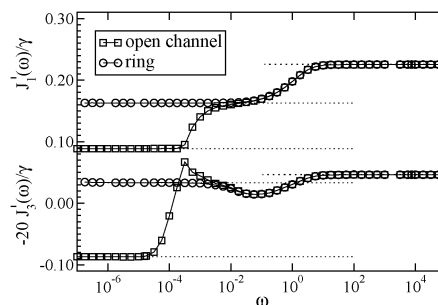


Fig. 7 First order and third order harmonics of the current in the ring and open channel for $\Delta U = 2$, $M = 2000$ and the exponential jump rates ($\mu_L = \mu_R = -1$ and $U_{0,1} = U_{M,M+1} = 2$ for the open channel). The results have been averaged over the same sets of 5 realizations of barrier disorder and the single-particle number in the open channel. The dotted lines mark the limiting behavior for high and low frequency (see text).

the low-frequency regime, where $J'_1(\omega)$ again becomes independent of ω . The third order harmonics $J'_3(\omega)$ in the ring also shows a plateau at high and low frequencies, and passes through a minimum in the dispersive regime. The plateau values in the limits of high and low frequencies follow from eqn (34) and (35), respectively, and are marked by dotted lines in the Figure. With respect to the imaginary parts $J''_1(\omega)$ and $J''_3(\omega)$, we found peaks appearing in the dispersive regimes in Fig. 7.

In the open channel the harmonics follow those in the ring system for higher frequencies. This can be understood from the fact that at higher frequencies the dynamics in the interior of the channel is dominant (“bulk behavior”). At lower frequencies, however, the coupling to the reservoirs leads to significant changes in the mean particle number. As a consequence, an additional dispersive regime³⁶ is seen at low frequencies, until the limit corresponding to eqn (35) is reached. Note in particular that $J'_3(\omega)$ changes its sign when approaching the low-frequency limit.

Let us finally note that we have obtained a similar overall behavior of the harmonics in the case of the box distribution of uncorrelated site energies disorder except of one notable difference: no change of sign in $J'_3(\omega)$ was observed in this case. It is interesting to note that for a site energy landscape with point symmetry and a bimodal distribution a change of sign of $J'_3(\omega)$ was found.²³ Hence, one can conclude that the occurrence of a change of sign of $J'_3(\omega)$ depends on details of the energy landscape.

6. Summary and conclusions

The problem of one-dimensional hopping transport has gained renewed interest, in particular in connection with biophysical charge carrier transport and with molecular electronic conduction. In this work we have discussed the situation for non-interacting particles, focusing on disorder effects (or regular variations of site and barrier energies) on the current response to an external bias. For both periodic ring and open channel systems, analytical results were derived for the stationary current in response to static external driving forces, without making specific assumptions on the form of the jump rates. Representative results were shown for spatially uncorrelated energy landscapes, characterized by box distributions either in the barrier or site energies.

It was further shown that in the ring system rectification effects become smaller for increasing system size. In the thermodynamic limit of infinite system size, the current $J_{dc}(u)$ becomes antisymmetric with respect to the bias u and its expansion in powers of u can exhibit non-analyticities of the form $|u|^{2n+1}u$, $n = 0, 1, \dots$. In open channels, rectification does not vanish in the thermodynamic limit due to the fact that the current is dominated by the variations of the energy landscape close to either system boundary, in a way that depends on the bias direction. It would be interesting to check this rectification effect in experiments, as, for example, in measurement of ionic currents in electrolytes in contact with non-blocking electrodes.

Numerical solutions of the underlying rate equations were obtained for a sinusoidal external driving force and results

were presented for the first and higher harmonics of the current. For intermediate and high frequencies the harmonics in the open channel were shown to equal those in the ring, if the particle concentration is adapted properly. In the low-frequency regime the harmonics can be derived from the quasistatic limit. This implies that the low-frequency limit is different in open channels and in rings. The origin of this difference can be attributed to changes in the mean particle number in the open system, which are absent in the ring model.

The results presented here provide a basis for further investigations of interacting particles. As discussed in section 4, in truly one-dimensional geometries hard-core interactions can already change the general characteristics of the transport behavior due to boundary induced phase transitions of the mean particle concentration. Influences of disorder effects on these phase transitions have been discussed in various works (see *e.g.* ref. 37–39), but a thorough general treatment for arbitrary disorder has yet not been provided. Only a few studies have been performed for longer range particle–particle interactions. An example is the treatment of nearest-neighbor repulsions in TASEPs on the basis of specific rules for the transition rates.^{40,41} This can give rise to more complex phase diagrams compared to the case of hard-core interactions. A more complete exploration of the effects of disorder and particle–particle interactions, as required to get a more detailed description of real systems, still remains an open challenge.

Acknowledgements

We thank W. Dieterich for very valuable discussions. Parts of this work were supported by the HI-CONDELEC EU STREP project (NMP3-CT-2005-516975) and the Israel-Niedersachsen Research Fund.

References

- 1 A. Nitzan and M. A. Ratner, *Science*, 2003, **300**, 1384.
- 2 A. Nitzan, *Annu. Rev. Phys. Chem.*, 2001, **52**, 681.
- 3 P. Romano, A. Polcari, B. Verrusco, V. Colantuoni, W. Saldarriaga and E. Baca, *J. Appl. Phys.*, 2007, **102**, 103720.
- 4 B. Xu, P. Zhang, X. Li and N. Tao, *Nano Lett.*, 2004, **4**, 1105.
- 5 B. Hille, *Ion Channels of Excitable Membranes*, Sinauer Associates, Sutherland, Massachusetts, 2001.
- 6 S. Berneche and B. Roux, *Nature*, 2001, **414**, 73; S. Berneche and B. Roux, *Proc. Natl. Acad. Sci. U. S. A.*, 2003, **100**, 8644.
- 7 P. Graf, M. G. Kurnikova, R. D. Coalson and A. Nitzan, *J. Phys. Chem. B*, 2004, **108**, 2006.
- 8 C. T. MacDonald, J. H. Gibbs and A. C. Pipkin, *Biopolymers*, 1968, **6**, 1.
- 9 E. Frey and K. Kroy, *Ann. Phys.*, 2005, **14**, 20, cond-mat/0502602.
- 10 H. Spohn, *Large Scale Dynamics of Interacting Particles*, Springer, New York, 1981.
- 11 B. Derrida and M. Evans, in *Nonequilibrium Statistical Mechanics in One Dimension*, ed. V. Privman, Cambridge University Press, Cambridge, 1997, ch. 14, pp. 277–304.
- 12 G. Schütz, in *Phase Transitions in Critical Phenomena*, ed. C. Domb and J. Lebowitz, Academic Press, San Diego, 2001, vol. 19, pp. 3–251.
- 13 A. Zilman, *Biophys. J.*, 2009, **96**, 1235.
- 14 P. Kohli, C. C. Harell, Z. Cao, R. Gasparac and R. Martin, *Science*, 2004, **305**, 984.
- 15 T. E. Harris, *J. Appl. Probab.*, 1965, **2**, 323.

- 16 H. van Beijeren, K. W. Kehr and R. Kutner, *Phys. Rev. B: Condens. Matter*, 1983, **28**, 5711.
- 17 M. Kollmann, *Phys. Rev. Lett.*, 2003, **90**, 180602.
- 18 K. W. Kehr, K. Mussawisade, T. Wichmann and W. Dieterich, *Phys. Rev. E: Stat. Phys., Plasmas, Fluids, Relat. Interdiscip. Top.*, 1997, **56**, R2351.
- 19 V. Ambegaokar and B. I. Halperin, *Phys. Rev. Lett.*, 1969, **22**, 1364.
- 20 B. Roling, *Phys. Chem. Chem. Phys.*, 2001, **3**, 5093.
- 21 S. Murugavel and B. Roling, *J. Non-Cryst. Solids*, 2005, **351**, 2819.
- 22 A. Heuer, S. Murugavel and B. Roling, *Phys. Rev. B: Condens. Matter Mater. Phys.*, 2005, **72**, 174304.
- 23 B. Roling, S. Murugavel, A. Heuer, L. Lühning, R. Friedrich and S. Röthel, *Phys. Chem. Chem. Phys.*, 2008, **10**, 4211.
- 24 M. Kunow and A. Heuer, *J. Chem. Phys.*, 2006, **124**, 214703.
- 25 N. Mott and E. Davis, *Electronic Processes in Non-Crystalline Materials*, Clarendon, London, 1979.
- 26 P. Maass, in Periodic Activity Report of the EU STREP project HI-CONDELEC (NMP3-CT-2005-516975), May, 2006.
- 27 In ref. 23, some numerical results were presented for spatially uncorrelated site energies with a bimodal distribution under the constraint of point symmetry.
- 28 R. J. Glauber, *J. Math. Phys.*, 1963, **4**, 294.
- 29 P. Maass, B. Rinn and W. Schirmacher, *Philos. Mag. B*, 1999, **79**, 1915.
- 30 J.-F. Gouyet M. Plapp, W. Dieterich and P. Maass, *Adv. Phys.*, 2003, **52**, 523.
- 31 Considering an ordered system ($e_i = 0$, $U_i = \text{const.}$) with a bias $u \neq 0$ and taking the continuum limit of eqn (25),(26), the mean-field bulk current is given by $j_b = j_{dr} + j_D$ with a drift current $j_{dr} = 2\Delta\Gamma\rho(1 - \rho)$ and a diffusive current $j_D = -\partial_x[D(\rho)\rho]$, where ρ is the particle concentration, $D(\rho) = \bar{\Gamma}[1 - (1 - \rho)\Delta\Gamma/\bar{\Gamma}] > 0$ and $\bar{\Gamma} = (\Gamma^+ + \Gamma^-)/2$, $\Delta\Gamma = (\Gamma^+ - \Gamma^-)/2$. The diffusion profile $\rho_{st} = \rho_{st}(x)$ in the stationary state then follows uniquely from $j_b = j_{st}$, when taking into account the boundary conditions $j_L = j_R = j_{st}$ connected with the boundary currents $j_L = (\bar{\Gamma}_L + \Delta\Gamma_L) - 2\bar{\Gamma}_L\rho_L$ and $j_R = (\bar{\Gamma}_R + \Delta\Gamma_R) - 2\bar{\Gamma}_R\rho_R$, where $\rho_L = \rho(0)$ and $\rho_R = \rho(\tilde{M})$ are the boundary densities (with $\tilde{M} = Ma$ the channel length) and $\bar{\Gamma}_{L,R} = (\Gamma_{L,R}^+ + \Gamma_{L,R}^-)/2$, $\Delta\Gamma_{L,R} = (\Gamma_{L,R}^+ - \Gamma_{L,R}^-)/2$. The analysis yields 3 different phases, where in each of these the mean particle concentration $\rho_{st} = \lim_{L \rightarrow \infty} \{\int_0^L dx \rho_{st}(x)/L\}$ in the stationary state and thermodynamic limit equals one of three possible values. For $\Delta\Gamma > 0$ these are $\bar{\rho}_{st} = \rho_L$ (for $\rho_L < 1 - \rho(L)$ and $\rho_L < 1/2$), $\bar{\rho}_{st} = \rho_R$ (for $\rho_L > 1 - \rho_R$ and $\rho_R > 1/2$), or $\bar{\rho}_{st} = 1/2$ (for $\rho_L > 1/2$ and $\rho_R < 1/2$); for further details, see e.g.ref. 32.
- 32 B. Derrida, *Phys. Rep.*, 1998, **301**, 65.
- 33 The set of eqn (25),(28) is, of course, intuitive and one may use it as a starting point of a phenomenological description without referring to its derivation from the fermionic lattice gas. In such phenomenological approach one would not necessarily require the p_i to be much smaller than one. Indeed, we found that due to the linearity of the equations of motions, this restriction is not relevant with respect to the overall qualitative behavior of the system. However, application of these equations to situations with p_i not being much smaller than one should be considered with care.
- 34 S. Datta, *Quantum Transport: Atom to Transistor*, Cambridge University Press, Cambridge, 2005.
- 35 This does no longer hold true in the case of energy disorder so that a more sophisticated treatment has to be performed in this case.
- 36 For stronger disorder, different system sizes and different chemical potentials the onset frequency, where the behavior in the open channel starts to deviate from the behavior in the ring, can be shifted.
- 37 G. Tripathy and M. Barma, *Phys. Rev. Lett.*, 1997, **78**, 3039.
- 38 R. J. Harris and R. B. Stinchcombe, *Phys. Rev. E: Stat., Nonlinear, Soft Matter Phys.*, 2004, **70**, 016108.
- 39 M. R. Evans, T. Hanney and Y. Kafri, *Phys. Rev. E: Stat., Nonlinear, Soft Matter Phys.*, 2004, **70**, 066124.
- 40 J. Krug, *Phys. Rev. Lett.*, 1991, **67**, 1882.
- 41 J. S. Hager, J. Krug, V. Popkov and G. M. Schütz, *Phys. Rev. E: Stat., Nonlinear, Soft Matter Phys.*, 2001, **63**, 056110.